RSC Advances

PAPER

View Article Online
View Journal | View Issue

Check for updates

Cite this: *RSC Adv.*, 2023, **13**, 7020

# Synthesis and characterization of hydroxyl-terminated polybutadiene modified low temperature adaptive self-matting waterborne polyurethane

Jiaran Liu, Desheng Yang, Shengnan Li, Chaofei Bai, Chengzhao Tu, Fengdan Zhu, Wei Xin, Guoping Li * and Yunjun Luo

Hydroxyl-terminated polybutadiene (HTPB) is a flexible telechelic compound with a main chain containing a slightly cross-linked activated carbon–carbon double bond and a hydroxyl group at the end. Therefore, in this paper, HTPB was used as a terminal diol prepolymer, and sulfonate AAS and carboxylic acid DMPA were used as hydrophilic chain extenders to prepare low-temperature adaptive self-matting waterborne polyurethane (WPU). Due to the fact that the non-polar butene chain in the HTPB prepolymer cannot form a hydrogen bond with the urethane group, and the solubility parameter difference between the hard segment formed by the urethane group is large, the gap of $T_g$ between the soft and hard segments of the WPU increases by nearly 10 °C, with more obvious microphase separation. At the same time, by adjusting the HTPB content, WPU emulsions with different particle sizes can be obtained, thereby obtaining WPU emulsions with good extinction properties and mechanical properties. The results show that HTPB-based WPU with a certain degree of microphase separation and roughness obtained by introducing a large number of non-polar carbon chains has good extinction ability, and the 60° glossiness can be as low as 0.4 GU. Meanwhile, the introduction of HTPB can improve the mechanical properties and low temperature flexibility of WPU. The $T_{g,s}$ (the glass transition temperature of soft segment) of WPU modified by the HTPB block decreased by 5.82 °C, and the $\Delta T_g$ increased by 21.04 °C, indicating that the degree of microphase separation increased. At −50 °C, the elongation at break and tensile strength of WPU modified by HTPB can still maintain 785.2% and 76.7 MPa, which are 1.82 times and 2.91 times those of WPU with only PTMG as soft segment, respectively. The self-matting WPU coating prepared in this paper can meet the requirements of severe cold weather and has potential application prospects in the field of finishing.

Received 19th January 2023
Accepted 22nd February 2023

DOI: 10.1039/d3ra00412k

rsc.li/rsc-advances

Open Access Article. Published on 01 March 2023. Downloaded on 6/19/2026 1:35:13 AM.
This article is licensed under a Creative Commons Attribution-NonCommercial 3.0 Unported Licence.

## 1. Introduction

With the change of people's aesthetic concepts, low gloss coatings are becoming more and more popular in surface decoration and architectural design.[1] Compared with high gloss coatings, low gloss coatings are suitable for hiding minor scratches and defects, reducing dust and fingerprint aggregation.[2–6] They can also reduce visual distraction and make people more focused, such as reducing surface glare in schools and hospitals. Therefore, matt coatings are widely used on the surfaces of wood and furniture, leather accessories, automotive parts, aircraft shells, electronic equipment shells, school and hospital wall surfaces and so on.[2,7–11] With the global emphasis on environmental protection concepts, volatile organic solvent (VOC) emission standards are becoming more and more stringent.[12–16] Waterborne polyurethane (WPU) is a polyurethane resin with water as dispersion medium.[11] WPU not only has the advantages of traditional solvent-based polyurethane, such as excellent wear resistance and mechanical properties, but also is environmentally friendly, safe and reliable.[10,12,17] Therefore, it is widely used in coatings, adhesives, leather finishing agents and inks.[9,18,19]

The principle of obtaining low gloss coating is that the rough surface has microscopic protrusions and depressions. When the light is irradiated, the light will be reflected in different directions at different reflection angles to form a diffuse reflection, giving the impression of low gloss. For WPU resins, the change in refractive index is negligibly small and has a limited effect on gloss. Therefore, the method of reducing the gloss of different types of coatings depends on the control of surface morphology to a large extent. The fabricated rough morphology can scatter the incident light to multiple directions to achieve the extinction effect.[5] Traditional matting agents (silica, diatomite, *etc.*) are incompatible with WPU emulsions

*Beijing Institute of Technology, China. E-mail: girlping3114@bit.edu.cn*



© 2023 The Author(s). Published by the Royal Society of Chemistry

Open Access Article. Published on 01 March 2023. Downloaded on 6/19/2026 1:35:13 AM.
This article is licensed under a Creative Commons Attribution-NonCommercial 3.0 Unported Licence.

and cannot be completely dispersed, forming a rough surface during film formation. The disadvantage of the external matting agent is that the matting agent particles are not fixed firmly and are easily detached from the surface. The rough structure will disappear over time, and the extinction effect will decrease. In addition, the added matting agent will reduce the stability of the emulsion and the bending resistance of the coating.[3,20–23] Self-matting WPU does not contain any additional matting agent, but generates emulsion particles with similar effects to matting agent during the synthesis process. When film-forming these emulsion particles mutually accumulate to form micro-rough surfaces, to achieve extinction effect. When the solvent evaporates, these emulsion particles accumulate with each other to form a microscopically rough surface, achieving a matting effect. Therefore, self-matting WPU has better emulsion stability. At the same time, it eliminates the defects caused by the use of matting agent, and also improves the mechanical properties and water resistance of WPU matte coating. It has the advantages of environmental protection and low cost.[3,20–23]

The particle size of WPU can be easily adjusted through formula adjustment.[7] In order to obtain a stable WPU lotion, hydrophilic groups (carboxylic acid and sulfonic acid, amine) are usually added to the main chain or side chain of the polymer.[8] Li *et al.*[21] prepared WPU using amino sulfonate chain extender (A95) and hydrazine hydrate as both chain extender and emulsifier. The WPU lotion particles obtained were formed regular microspheres. The 60° gloss of the coating film was as low as 1.5 GU. Yong *et al.*[1] synthesized a new solvent-free WPU dispersion using AAS and DMPA as hydrophilic chain extenders. AAS can provide better hydrolysis stability and thermal stability of the coating than DMPA. It avoids the excessive use of DMPA in the process of improving the glossiness and water resistance of WPU coating. At the same time, AAS is instrumental in the formation of many regular spherical particles in WPU lotion. Moreover, the increase of the content of sulfonic acid hydrophilic chain extender or the initial molecular weight of the soft segment is beneficial to the improvement of thermal stability. Cao *et al.*[20] introduced trimethylolpropane (TMP) and AAS salt into the polyurethane prepolymer as the post chain extender. TMP has the function of improving the micro phase separation and reducing the loss factor. By increasing the micro phase separation between the hard segment and the soft segment of polyurethane, it can form relief to increase the roughness of the coating. Yong *et al.*[2] precisely adjusted the surface roughness of the film by changing the weight ratio of the hard/soft monomer of the acrylic monomer, and the gloss of the WPU acrylate (WPUA) hybrid lotion coating obtained can be as low as 3 GU. Some researchers are also working on more complex technologies. Bauer *et al.*[24] used a dual ultraviolet lamp device (consisting of 172 nm excimer lamp and mercury arc lamp) to irradiate the acrylate formula to form a micro texture morphology, resulting in a low gloss or matte effect of the film.

However, the research on self extinction WPU mainly focuses on improving the extinction ability at present, and the research on the mechanical properties and water resistance of WPU, especially the mechanical properties at low temperature, is rare. HTPB is one of the liquid rubbers, which has a long non-polar carbon chain. Because of its low glass transition temperature, high elasticity, high water resistance and hydrophobicity, HTPB is widely used in adhesives, foam, rocket propellant and other fields.[25,26] The low surface energy and flexibility at low temperature of HTPB based polyurethane elastomers have been extensively studied,[27,28] however, there are few studies on HTPB based WPU resins. Ding *et al.*[3] proposed a method to exfoliate organic montmorillonite into single-layer nanosheets in HTPB, and then reacted with isocyanate to synthesize a multifunctional matte WPU coating. The nanosheets promoted the crosslinking and cyclization of HTPB at high temperature, making the surface morphology of the coating rougher. In the matte range, the 60° gloss is reduced to 4.6 GU.

In this paper, HTPB was introduced into the main chain, together with PTMG as soft segment. At the same time, DMPA and AAS containing hydrophilic groups were introduced as chain extender and emulsifier, and then EDA was used to extend the chain. And the low gloss WPU with low temperature adaptability was successfully prepared. By adjusting the HTPB content to adjust the particle size of the emulsion, the extinction performance is greatly improved. At the same time, after HTPB was introduced into the WPU segment, the longer non-polar carbon chain in the HTPB structure will cause obvious microphase separation in the soft and hard segment regions,[14] thereby roughening the WPU film surface to achieve the effect of extinction. The extinction principle is shown in Fig. 1. In addition, the strong hydrophobic olefin bonds in HTPB can improve the water resistance of WPU. Due to the excellent elasticity and flexibility of HTPB, the mechanical properties and low temperature flexibility of WPU can be well improved, so that the self-matting WPU coating can meet the requirements of cold weather.

## 2. Materials and methods

### 2.1 Materials

The raw materials used in this study include poly(tetramethylene glycol) (PTMG, $(\overline{M_n}) = 2000$ g mol$^{-1}$), hydroxyl terminated polybutadiene (HTPB, $(\overline{M_n}) = 2000$, hydroxyl group content : 0.71 − 0.80 mmol g$^{-1}$), neopentyl glycol (NPG), isophorone diisocyanate (IPDI, used as received),

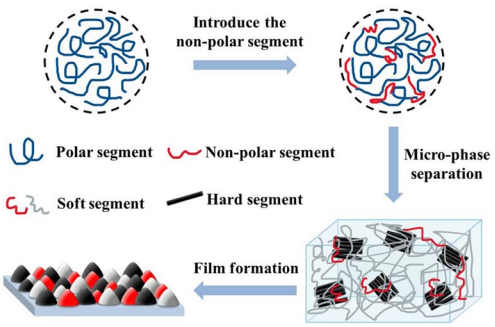


Fig. 1 Schematic diagram of extinction mechanism of HTPB modified waterborne polyurethane extinction resin.

Open Access Article. Published on 01 March 2023. Downloaded on 6/19/2026 1:35:13 AM.
This article is licensed under a Creative Commons Attribution-NonCommercial 3.0 Unported Licence.

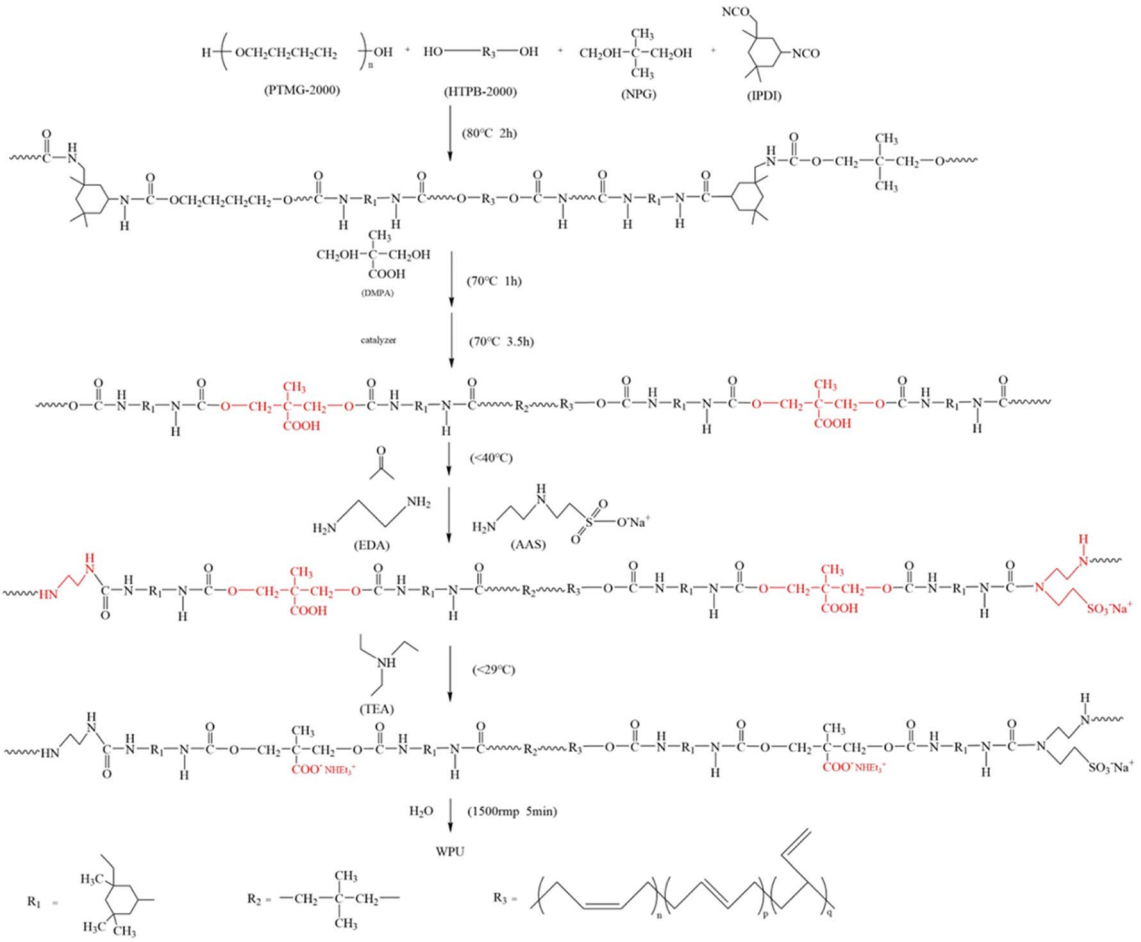


Scheme 1 Synthesis route of self-matting waterborne polyurethane.

2,2-bis(hydroxymethyl)propionic acid (DMPA), *N*-methylpyrrolidone (NMP), sodium 2-[(2-amino ethyl)amino]ethane sulfonate (AAS salt), ethylenediamine (EDA), trimethylamine (TEA), neodecanoic acid bismuth($3^+$) salt. All these raw materials were analytical reagents and purchased from Macklin Chemical Reagent Co. Ltd. (Shanghai, China).

### 2.2 Preparation of WPU

A certain amount of PTMG and HTPB were placed to a three neck flask and dehydrated in vacuum at 120 °C for 2 h. After cooling to 80 °C, NPG and IPDI were added by stirring for 2 h. The mixture was cooled to 70 °C and DMPA diluted with NMP was added to it for 1 h. Two drops of neodecanoic acid bismuth($3^+$) salt were added to the reaction system and the reaction was carried out for 3.5 h at 70 °C. The viscosity was adjusted with an appropriate amount of acetone. After the temperature of the reactor was maintained under 40 °C, AAS and EDA diluted with water were slowly added dropwise to the flask under vigorous stirring. After cooling to 29 °C, TEA was added to neutralize the carboxyl group for 5 min. Transfer the above prepolymer to a plastic beaker and set the speed to 1500 rpm to emulsify for 10 minutes. After standing overnight, acetone was removed by vacuum distillation. The emulsion was aged at 60 °C for 2–3 days to obtain the low-glossed WPU emulsion. The above reaction procedure is presented in Scheme 1. The formulations used are shown in Table 1 (WPU-B0% means the amount of HTPB added is 0%, and the meaning of WPU-B10–50% is the same).

### 2.3 Characterization

**2.3.1 FTIR-ATR.** The infrared absorption of waterborne polyurethane was tested by the 8700 Fourier transform infrared spectrometer (ATR-FTIR, Nicolet, USA). The sample was scanned 48 times at a resolution of 4 $cm^{-1}$ over the frequency range of 4000–400 $cm^{-1}$.

**2.3.2 Particle size and zeta potential test.** After emulsification, the particle size of WPU emulsion was carried out *via* a Zetasizer Nano ZS90 laser particle size tester from Malvern (Malvern, UK). The emulsion was diluted with deionized water to a mass fraction of 0.01% and measured at room temperature.

**2.3.3 Gloss test of self-matting WPU leather coatings.** 10 g WPU emulsion and 0.1 g wetting agent (BYK381) were mixed for 10 min, coated on the PVC leather using a 40 μm wire rod, and subsequently placed in an oven at 120 °C. After drying for 2 min, the leather samples were taken out for gloss test. According to GB/T9754-2007 "paints and varnishes – determination of 20°,


© 2023 The Author(s). Published by the Royal Society of Chemistry

Open Access Article. Published on 01 March 2023. Downloaded on 6/19/2026 1:35:13 AM.
This article is licensed under a Creative Commons Attribution-NonCommercial 3.0 Unported Licence.

Table 1 Formulation of self-matting waterborne polyurethane

| Sample | Block ratio (PTMG:HTPB) | PTMG:HTPB | Content of DMPA | Content of AAS | Hard segment content | Chain extension ratio | *R* value |
|---|---|---|---|---|---|---|---|
| WPU-B0% | — | 10 : 00 | 0.50% | 0.50% | 36% | 0.62 | 1 |
| WPU-B10% | 22.1 : 1 | 9 : 1 | | | | | |
| WPU-B20% | 9.8 : 1 | 8 : 2 | | | | | |
| WPU-B30% | 5.7 : 1 | 7 : 3 | | | | | |
| WPU-B40% | 3.7 : 1 | 6 : 4 | | | | | |
| WPU-B50% | 2.5 : 1 | 5 : 5 | | | | | |

60° and 85° specular gloss of paint films without metallic pigments", the 60° gloss was determined using the Ref 101N photometer from Sheen (Essex, UK). The average value of three tests was used as the final result.

**2.3.4 Stability test of WPU emulsion.** The stability of WPU emulsion was determined according to GB/T6753.3-1986 "test method for storage stability of coatings". Centrifuge emulsion of the same mass in a high-speed centrifuge (HC-3018) at a speed of 3000 rpm for 15 min. Observe the state of the emulsion. If there is no precipitation, it can be considered that the emulsion has a storage stability period of 6 months or more.

**2.3.5 Water contact angle of self-matting WPU leather coatings.** The static water contact angle of leather coating samples was measured at 25 °C with OCA20 contact angle tester (Dataphysics, Germany).

**2.3.6 Thermogravimetry (TG).** In a $N_2$ atmosphere, the thermal decomposition of the film was tested by a TGA/DSC1 type weight loss analyzer (Mettler Toledo, Switzerland) from 30 to 600 °C at a heating rate of 10 °C $min^{-1}$. Weight loss was recorded as a function of temperature.

**2.3.7 Differential scanning calorimetry (DSC).** Under the protection of $N_2$, the glass transition temperature ($T_g$) of the film was obtained by using a DSC1 differential scanning calorimeter from Mettler Toledo. The test range was −150 to 150 °C and the heating rate was 10 K $min^{-1}$.

**2.3.8 SEM.** A SU8020 scanning electron microscope (TESCAN MIRA LMS) was used to observe the surface morphology of the polyurethane coating film on the leather. The operating voltage was 3 kV, and gold was sprayed before the sample test to improve the conductivity.

**2.3.9 Tensile properties.** According to "GBT 528-1998 determination of tensile stress–strain properties of vulcanized rubber or thermoplastic rubber", cut the waterborne polyurethane film to a size of 2 mm × 12 mm dumbbell shaped standard spline. The tensile properties of the standard spline are tested by AGS-J electronic universal testing machine. The test temperature is 25 °C and −50 °C, and the tensile rate is 100 mm $min^{-1}$.

# 3. Results and discussion

## 3.1 Structural characterization of HTPB-based WPU

The ATR-FTIR spectra of raw materials and WPU film are shown in Fig. 2. Fig. 2 shows that the three raw materials have their own exclusive infrared characteristic absorption peaks. The peaks at 3470 $cm^{-1}$ and 1112 $cm^{-1}$ was caused by the stretching vibration of –OH and C–O–C in PTMG, respectively. The broad absorption peaks at 3200–3600 $cm^{-1}$ were attributed to the –OH of HTPB. The weak absorption peak at 726 $cm^{-1}$ was corresponding to the carbon–carbon double bond in the *cis*-1,4 conformation of HTPB. While there was a strong absorption peak of the bending vibration absorption peaks of carbon–carbon double bond in *trans*-1,4 conformation and 1,2-vinyl conformation of HTPB at 967 $cm^{-1}$ and 909 $cm^{-1}$. The stretching vibration of –NCO of IPDI located at 2264 $cm^{-1}$.

The peak at 1716 $cm^{-1}$ was attributed to the carbonyl absorption peak of carbamate bond. The peak at 3332 $cm^{-1}$ and 1548 $cm^{-1}$ was caused by the stretching vibration and bending vibration of N–H. And there was no characteristic absorption peak of –NCO of isocyanate at 2264 $cm^{-1}$, indicating that the isocyanate had been fully involved in the reaction. At the same time, the absorption peaks of carbon–carbon double bonds of HTPB can be seen at 726 $cm^{-1}$, 967 $cm^{-1}$ and 909 $cm^{-1}$, which shows that HTPB has been inserted into the WPU main chain successfully.[29,30] In addition, the absorption peaks at 2854–2941 $cm^{-1}$ were attributed to the C–H stretching vibration of –$CH_3$ and –$CH_2$. The IR spectrum demonstrated the aqueous polyurethane was synthesized.

## 3.2 Stability and particle size analysis of self-matting WPU dispersions

**3.2.1 Effect of HTPB addition on particle size of WPU.** The changes of particle size of WPU with different HTPB content are shown in Fig. 3. WPU emulsion without HTPB modification had

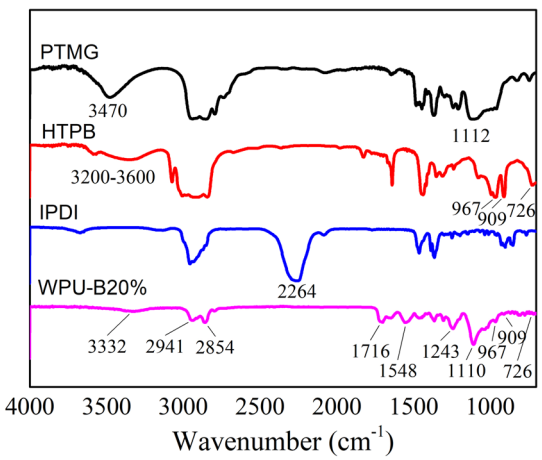


Fig. 2 ATR-FTIR spectra of raw materials and WPU.

Open Access Article. Published on 01 March 2023. Downloaded on 6/19/2026 1:35:13 AM.
This article is licensed under a Creative Commons Attribution-NonCommercial 3.0 Unported Licence.

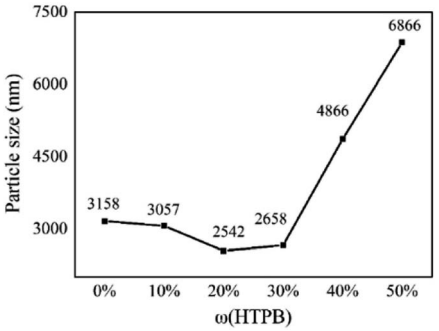


Fig. 3 The particle sizes of WPU dispersions with different HTPB content.

a particle size of 3158 nm. After HTPB was added, the particle size of the WPU emulsion decreased slightly and then increased gradually. When the amount of HTPB added was small, the hydrophobic segments in the emulsion will be agglomerated and wrapped in the interior of the ball by hydrophilic groups. At this time, the hydrophobic properties were not dominant. Therefore, the particle size didn't increase when the HTPB content was below 20%. There was an ether oxygen bond between each monomer in the molecular structure of PTMG, while the molecular structure of HTPB was a double bond but no ether oxygen bond. The ether oxygen bond in the product synthesized by PTMG can form intermolecular hydrogen bonds. When PTMG was replaced by a small part of HTPB, the ether oxygen bond was reduced. Therefore, the intermolecular force was weakened to a certain extent, and the physical crosslinking points in and between the macromolecular chains were reduced. Due to the low speed of emulsification, the intermolecular force was difficult to be broken when the amount of HTPB was small. In consequence, it is easy to be sheared and dispersed when emulsified in water, and the particle size of the emulsion is slightly reduced.

When the addition of HTPB continues to increase, the average particle size of WPU emulsions was significantly affected by the hydrophilicity of WPU. The block ratio of the sample with HTPB content of 50% is 2.5 : 1, and the average particle size of the emulsion reached a maximum of 6866 nm. HTPB structure is composed of full carbon chain, which is not hydrophilic. Therefore, as the HTPB content increased, the hydrophilicity of the whole system decreased, although the content of the hydrophilic chain extender (DMPA, AAS) of the system remained constant. Consequently, the water dispersibility of the emulsion became worse, which led to an increase in the average particle size of the emulsion. In addition, the carbon–carbon double bonds in HTPB molecules existed in three forms, namely *cis*-1,4 structure, *trans*-1,4 structure and 1,2-vinyl structure. These irregular structures made it unable to be closely arranged to form a relatively large spatial structure.[31] These two factors led to the increase of the average particle size of the emulsion when the HTPB content increased.

**3.2.2 Appearance and stability of WPU dispersions.** The appearance, centrifugal stability and zeta potential of WPU emulsions with different HTPB contents are shown in Table 2. The emulsion looked opaque and milky white. The emulsion was centrifuged with only a few re-dispersed precipitates when the HTPB content was 0–30%. And the absolute value of the zeta potential is greater than 30 mV, so there was a good storage stability of the emulsion. When the HTPB content reached 40% or more, a large amount of precipitation occurred after centrifugation, indicating that the emulsion couldn't be stably stored. The reason for the change of emulsion appearance and stability was that the hydrophobicity of molecular structure in HTPB structure made the hydrophilicity of WPU worse.

### 3.3 Room and low-temperature mechanical tensile properties of self-matting WPU film

The stress–strain curves of WPU with different HTPB content at room temperature are shown in Fig. 4. The data of tensile strength and elongation at break of WPU films with different HTPB content are shown in Table 3. It can be seen that with the increase of HTPB content, the tensile strength and elongation at break of WPU film increased first and then decreased. The tensile strength of WPU-B0% spline without HTPB was 20.6 MPa and the elongation at break was 1473.6%. When the HTPB content was 20%, the elongation at break of WPU-B20% was up to 1768.8%, and the tensile strength was 22.3 MPa. WPU-B40% had the highest tensile strength of 26.6 MPa and the elongation at break was 1354.9%.

The stress–strain curves of WPU film with different HTPB contents at −50 °C are shown in Fig. 5. It can be seen that the tensile strength of WPU-B0% spline without HTPB was 26.4 MPa and the elongation at break was 430.4% at −50 °C. After the introduction of HTPB, the tensile strength and elongation at break of WPU splines at low temperature were greatly improved. The elongation at break of WPU-B20% at −50 °C was

Table 2 Appearance and stability of WPU dispersions with different HTPB content

| Sample | Appearance of emulsion | Centrifugal stability | Zeta potential/mV |
|---|---|---|---|
| WPU-B0% | Opaque, milky white | Small amount of precipitate, re-dispersible | −63.5 |
| WPU-B10% | Opaque, milky white | Small amount of precipitate, re-dispersible | −74.3 |
| WPU-B20% | Opaque, milky white | Small amount of precipitate, re-dispersible | −50.4 |
| WPU-B30% | Opaque, milky white | Small amount of precipitate, re-dispersible | −54.5 |
| WPU-B40% | Opaque, milky white | Large amount of precipitate, re-dispersible | −57.7 |
| WPU-B50% | Opaque, milky white | Large amount of precipitate, re-dispersible | −51.6 |


© 2023 The Author(s). Published by the Royal Society of Chemistry

Open Access Article. Published on 01 March 2023. Downloaded on 6/19/2026 1:35:13 AM.
This article is licensed under a Creative Commons Attribution-NonCommercial 3.0 Unported Licence.

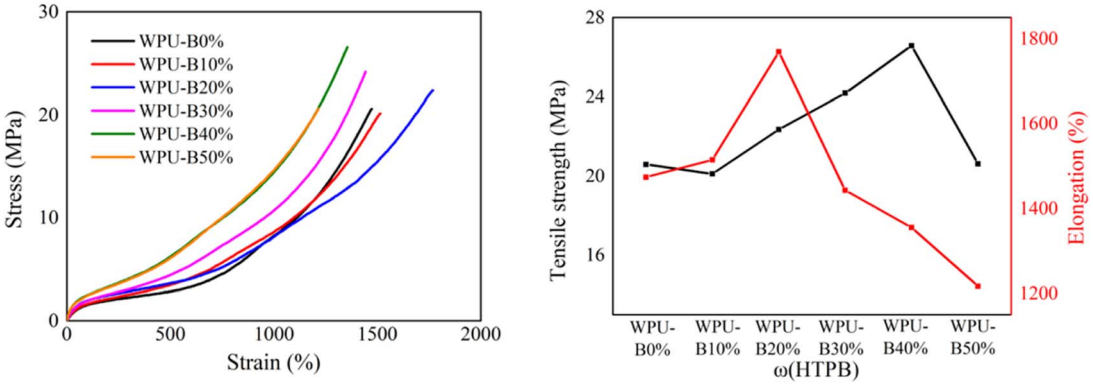


Fig. 4 The stress–strain curves of WPU films with different HTPB contents at 25 °C.

Table 3 Tensile strength and elongation at break of WPU film with different HTPB content at 25 °C and 50 °C

| | 25 °C | | −50 °C | |
|---|---|---|---|---|
| ω(HTPB) | Tensile strength (MPa) | Elongation (%) | Tensile strength (MPa) | Elongation (%) |
| WPU-B0% | 20.6 | 1473.6 | 26.4 | 430.4 |
| WPU-B10% | 20.1 | 1514.6 | 65.0 | 699.8 |
| WPU-B20% | 22.3 | 1768.8 | 76.7 | 785.2 |
| WPU-B30% | 24.2 | 1443.1 | 73.5 | 757.4 |
| WPU-B40% | 26.6 | 1354.9 | 47.0 | 667.5 |
| WPU-B50% | 20.6 | 1216.7 | 48.4 | 727.6 |

785.2% and the tensile strength was 76.7 MPa. The increase of HTPB content increased the holistic soft segment content and improved the flexibility of the molecular chain.

The significant improvement of mechanical properties after adding HTPB was mainly attributed to the structure of HTPB. Due to the difference in polarity, the soft and hard segments in WPU would aggregate with each other to produce microphase separation. The main chain of HTPB was composed of long non-polar carbon chains. The introduction of HTPB weakened the hydrogen bonding between soft and hard segments, which aggravated the microphase separation between soft and hard segments. The weakening of the interaction between soft and hard segments made the hard segments distribute freely in soft segments, which played the role of physical crosslinking point and could improve the tensile strength of WPU. The increase of HTPB content also increased the integral soft segment content, thereby improving the flexibility of the molecular chain and increasing its elongation under stress. Therefore, appropriate increase of microphase separation was beneficial to improve the tensile strength and elongation at break simultaneously. However, when the HTPB content was 50%, the further increase of microphase separation led to a sharp decline in the interaction between the soft and hard segments of the WPU-B50% film, showing a discontinuous state. This resulted in a decrease in the tensile strength and elongation at break of the WPU-B50% film under stress.

### 3.4 Thermal analysis of WPU

**3.4.1 Microphase separation.** The DSC curve of WPU film with different HTPB content are shown in Fig. 6. The $T_g$ data of WPU films with different HTPB contents are listed in Table 4. Fig. 6 shows that all WPU samples had two glass transition temperatures, corresponding to the glass transition temperatures of the soft and hard segments of WPU, respectively. It showed that there was a certain microphase separation in the whole system. It could be seen from Table 4 that with the

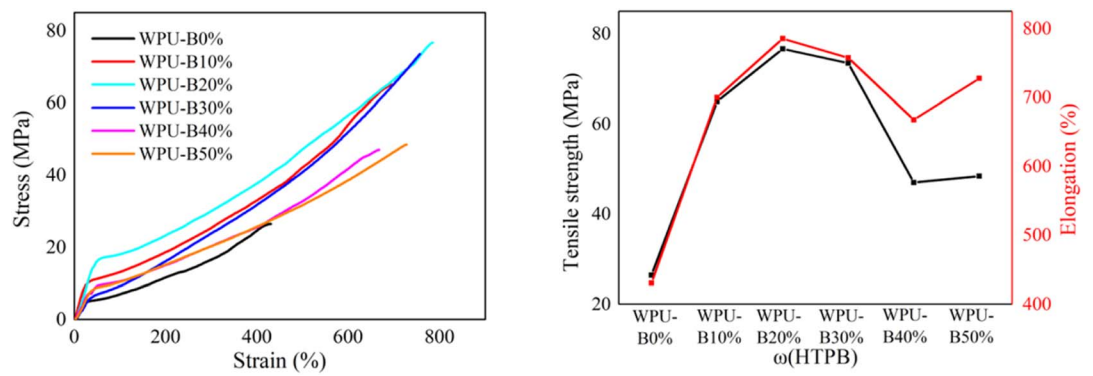


Fig. 5 The stress–strain curves of WPU films with different HTPB content at −50 °C.

Open Access Article. Published on 01 March 2023. Downloaded on 6/19/2026 1:35:13 AM.
This article is licensed under a Creative Commons Attribution-NonCommercial 3.0 Unported Licence.

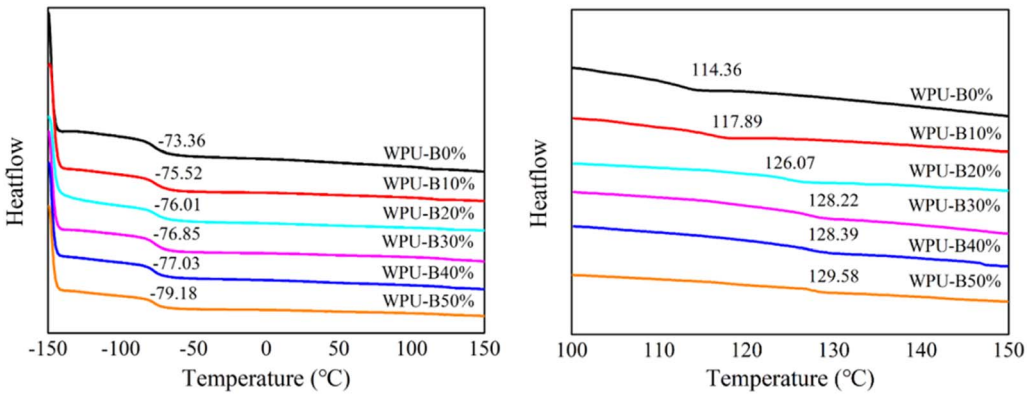


Fig. 6 DSC curves of WPU films with different HTPB contents.

Table 4 $T_g$ of WPU films with different HTPB contents

| Sample | $T_{g,s}$/°C | $T_{g,h}$/°C | $\Delta T_g$/°C |
|---|---|---|---|
| WPU-B0% | −73.36 | 114.36 | 187.72 |
| WPU-B10% | −75.52 | 117.89 | 193.41 |
| WPU-B20% | −76.01 | 126.07 | 202.08 |
| WPU-B30% | −76.85 | 128.22 | 205.07 |
| WPU-B40% | −77.03 | 128.39 | 205.42 |
| WPU-B50% | −79.18 | 129.58 | 208.76 |

increase of HTPB content, the glass transition temperature of soft segment ($T_{g,s}$) decreased and the glass transition temperature of hard segment ($T_{g,h}$) increased gradually, indicating that the degree of microphase separation between soft and hard segments increased. The main chain of HTPB was composed of non-polar carbon chains and couldn't form hydrogen bonds with hard segments. Therefore, with the increase of HTPB content, the restriction effect of hard segment on soft segment was weakened, and the soft segment was more likely to move when the temperature changes. $T_{g,s}$ moved to the low temperature direction, which improved the low temperature flexibility of WPU.[32] At the same time, the interaction between the hard segments was enhanced by hydrogen bonding, so that the cohesive energy between the hard segments was increased. It's conducive to the formation of short-range ordered structure, resulting in $T_{g,h}$ moving to high temperature. As $T_{g,s}$ decreased and $T_{g,h}$ increased, the difference between $\Delta T_g$ increased, indicating that the degree of microphase separation between hard and soft segments gradually increased. It further explained that the changes of gloss, surface morphology, transmittance and mechanical properties of the film were caused by the increase of microphase separation.

**3.4.2 Thermal stability.** It can be seen from Fig. 7 that the thermal decomposition of WPU films with different HTPB contents mainly occurred in the range of 200–500 °C, and the residual mass of the samples remained basically constant after 500 °C. The thermal decomposition of WPU-B0% film without WPU modification was divided into three stages, corresponding to the decomposition of DMPA-TEA salt (200–270 °C), the decomposition of hard segment carbamate bonds (270–350 °C) and the decomposition of soft segment polyether (350–500 °C). For WPU modified by HTPB, in addition to the above three thermal decomposition stages, there was a decomposition stage between 450–500 °C, which was the thermal decomposition of HTPB. With the increase of HTPB content, the decomposition peak of HTPB between 450–500 °C gradually became obvious.

The decomposition temperature and carbon residue of WPU film at 5% and 50% weight loss are listed in Table 5. For WPU-0%, the ambient temperatures at 5% and 50% weight loss were

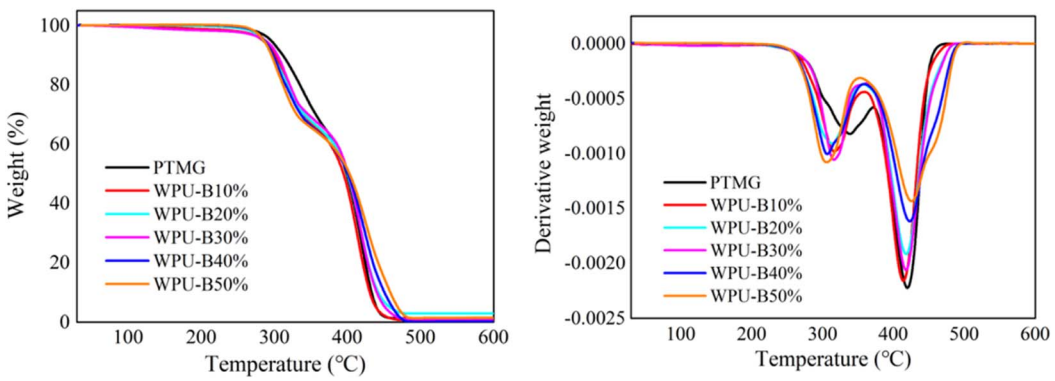


Fig. 7 TG, DTG curves of WPU films with different HTPB contents.


© 2023 The Author(s). Published by the Royal Society of Chemistry

Open Access Article. Published on 01 March 2023. Downloaded on 6/19/2026 1:35:13 AM.
This article is licensed under a Creative Commons Attribution-NonCommercial 3.0 Unported Licence.

Table 5 Decomposition temperature of WPU with different HTPB content at weight loss of 5% and 50% and carbon residue

| Sample | T5%/°C | T50%/°C | Carbon residue/% |
|---|---|---|---|
| WPU-B0% | 439.8 | 398.7 | 0.9 |
| WPU-B10% | 439.1 | 394.6 | 0.6 |
| WPU-B20% | 458.4 | 400.0 | 0.7 |
| WPU-B30% | 451.6 | 401.1 | 0.4 |
| WPU-B40% | 461.7 | 400.7 | 0.2 |
| WPU-B50% | 469.0 | 402.8 | 0.8 |

439.8 °C and 398.7 °C. The decomposition temperature of the samples after adding HTPB was greatly improved at 5% and 50% weight loss. The ambient temperatures of WPU-50% at 5% and 50% weight loss were 469.0 °C and 402.8 °C. It shows that the addition of HTPB can improve the thermal stability of WPU to a certain extent. In addition, there was only a small amount of residual carbon (less than 1%) left in all samples at 600 °C. There are a lot of C=C bonds in the main chain of HTPB molecular structure, and the bond energy of C=C bonds (615 kJ $mol^{-1}$) is much higher than that of C–O bonds (351 kJ $mol^{-1}$) and C–C bonds (348 kJ $mol^{-1}$) in PTMG molecular chain. The greater the bond energy, the greater the energy released when the chemical bond is formed, meaning that the chemical bond is more stable. Therefore, HTPB itself has good thermal stability, and the increase of HTPB content can improve the overall thermal stability. Moreover, due to the small C–H bond energy on HTPB allyl groups, allyl hydrogen was easily attacked by oxygen to form hydroperoxide and decompose into free radicals. Then further crosslinking reaction occurred between free radicals, resulting in a certain crosslinking in the WPU system. This crosslinking effect made the overall structure more compact, which limited and hindered the movement of WPU molecular chain segments to a certain extent and improved heat resistance.

### 3.5 Gloss analysis of self-matting WPU leather coating

The WPU leather coatings with different HTPB content and their 60° gloss with HTPB content are shown in Fig. 8. The extinction effect was excellent when the addition amount of HTPB was 0–20%. The gloss of WPU film was less than 1 GU, and the minimum was 0.4 GU. Since the addition of non-polar HTPB would increase the microphase separation between the soft and hard segments in WPU, the soft and hard segments were aggregated during the film formation process, changing the structure of the WPU film surface and resulting in changes in gloss. When the amount of HTPB was further increased, the microphase separation was too large to destroy the original surface structure, and thus the glossiness adversely increased to 3.3 GU.

The SEM images of WPU films with different HTPB additions are shown in Fig. 9. With the increase of HTPB content, the surface roughness of WPU film increased gradually and then tended to be smooth. The change of surface morphology of

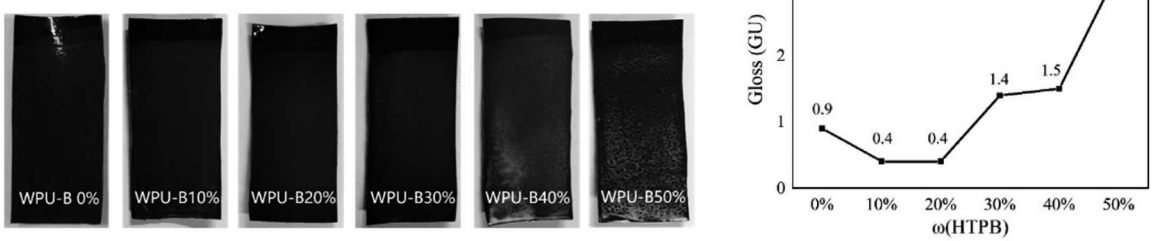


Fig. 8 Leather coating and gloss of WPU with different HTPB content.

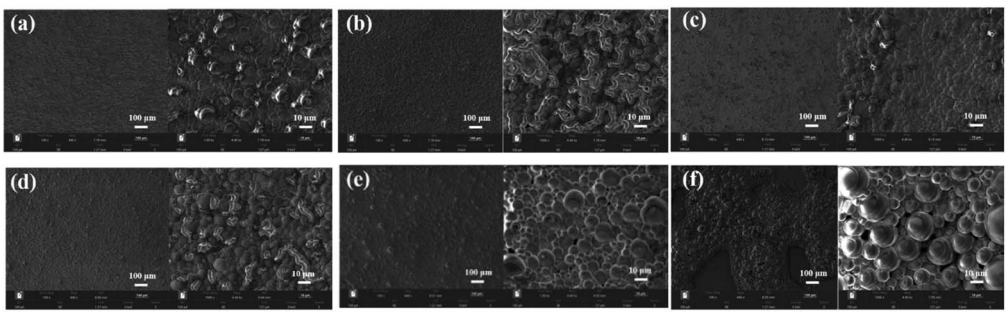


Fig. 9 SEM image of WPU coating surface with different HTPB content: (a) WPU-B0% (b) WPU-B10% (c) WPU-B20% (d) WPU-B30% (e) WPU-B40% (f) WPU-B50%.

Open Access Article. Published on 01 March 2023. Downloaded on 6/19/2026 1:35:13 AM.
This article is licensed under a Creative Commons Attribution-NonCommercial 3.0 Unported Licence.

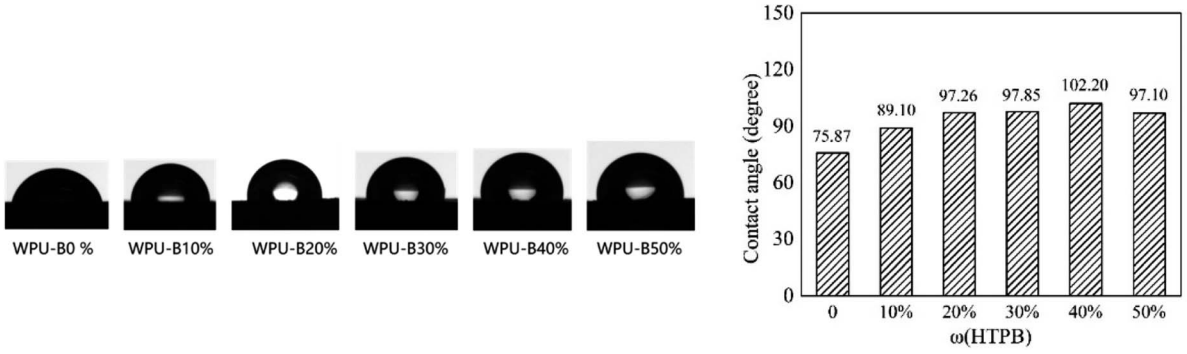


Fig. 10 Contact angle of WPU leather coating with different HTPB content.

WPU film was essentially determined by the degree of microphase separation in the system. The introduction of non-polar HTPB promoted the microphase separation between the soft and hard segments in WPU, resulting in the aggregation of the soft and hard segments in the WPU emulsion during the film forming process. After the emulsion was completely dried, incompatible two phases appeared on the surface of the film, forming different degrees of rough structure. When the degree of microphase separation was too small, it was not conducive to the formation of microspheres, such as WPU-B0% and WPU-B10%. Proper microphase separation produced more regular microsphere bulges, such as WPU-B20% and WPU-B30%. When the amount of HTPB continued to increase, the degree of microphase separation was too large, so that the hard segment was completely wrapped in the soft segment and the bulge couldn't be formed. Moreover, due to the large particle size, WPU couldn't be completely coated on the leather surface, resulting in increased gloss.

### 3.6 Water contact angle of self-matting WPU leather coating

Contact angle is a manifestation of the wetting phenomenon, which can directly reflect the hydrophilicity of the film surface and further support the water resistance of the film. The change of contact angle of WPU film with different HTPB content are shown in Fig. 10. When HTPB was not introduced into the soft segment, the contact angle of WPU-B0% was 75.85°. With the increase of HTPB content, the contact angle increased first and then decreased. This phenomenon indicated that the introduction of HTPB decreased the surface tension of WPU film and the surface hydrophobicity of WPU film was enhanced. Due to the existence of a large number of strong hydrophobic structures in the HTPB molecular chain, the more hydrophobic structures in the film will more effectively hinder the entry of water molecules. However, as shown in Fig. 9(f), when the addition amount of HTPB increased to 50%, the waterborne polyurethane emulsion could not be completely coated on the leather surface due to the large particle size. Since the uncoated part of the leather has not been hydrophobically modified, the contact angle value was slightly reduced.

## 4. Conclusion

In this paper, HTPB and PTMG were introduced as soft segments, and a combination of sulfonate and carboxyl hydrophilic chain extender was used to prepare a self-extinction WPU with excellent low temperature performance. After HTPB was introduced into the WPU segment, the longer non-polar carbon chain in the HTPB structure would cause obvious microphase separation in the soft and hard segment regions, resulting in a rough surface of the WPU film to achieve the effect of extinction. When the addition amount of HTPB was 20%, the particle size of the emulsion was about 2542 nm, and the gloss was as low as 0.4 GU. It had excellent extinction effect without additional matting agent. HTPB has excellent elasticity and flexibility, which can improve the mechanical properties and low temperature flexibility of WPU. The elongation at break at room temperature was up to 1768.8%, and the tensile strength was 22.3 MPa. The elongation at break could still be maintained at 785.2% at −50 °C, and the tensile strength was 76.7 MPa. So that the WPU coating meets the requirements of cold weather. At the same time, the self-matting WPU coating has excellent water resistance and good thermal stability. The prepared self-matting WPU has potential application prospects in the field of low gloss leather finishing.

## Conflicts of interest

There are no conflicts to declare.

## Acknowledgements

This work was supported by conventional and efficient destructive pre-research project (No. 7090201010115) and National Natural Science Foundation of China (No. 21905084). Here we expressed the heartfelt thanks for the support.

## References

1 Q. Yong, F. Nian, B. Liao, L. Huang, L. Wang and H. Pang, *RSC Adv.*, 2015, **5**, 107413–107420.


© 2023 The Author(s). Published by the Royal Society of Chemistry

Open Access Article. Published on 01 March 2023. Downloaded on 6/19/2026 1:35:13 AM.
This article is licensed under a Creative Commons Attribution-NonCommercial 3.0 Unported Licence.

2 Q. Yong, H. Pang, B. Liao, W. Mo, F. Huang, H. Huang and Y. Zhao, *Prog. Org. Coating*, 2018, **115**, 18–26.
3 Z. Ding, J. Li, W. Xin, G. Zhang and Y. Luo, *Prog. Org. Coating*, 2019, **136**, 105273.
4 Q. Yong and C. Liang, *Polymers*, 2019, **11**, 322.
5 Q. Yong, B. Liao, G. Ying, L. Caizhen, H. Huang and H. Pang, *J. Coat. Technol. Res.*, 2018, **15**, 993–1002.
6 Q. Yong, F. Nian, B. Liao, Y. Guo, L. Huang, L. Wang and H. Pang, *Polym. Bull.*, 2017, **74**, 1061–1076.
7 J. Zhu, H. Huang and X. Peng, *RSC Adv.*, 2016, **6**, 102368–102372.
8 C. Yu, C. Yan, J. Shao and F. Zhang, *Colloid Polym. Sci.*, 2021, **299**, 1489–1498.
9 Z. Wei, Z. Liu, X. Fu, Y. Wang, A. Yuan and J. Lei, *Eur. Polym. J.*, 2021, **157**, 110647.
10 L. Ren, C. Lin and P. Lei, Journal of, *J. Appl. Polym. Sci.*, 2021, **138**, 51382.
11 Y. Lai, Y. Qian, D. Yang, X. Qiu and M. Zhou, *Ind. Crops Prod.*, 2021, **170**, 113739.
12 Y. Qian, F. Dong, L. Guo, X. Xu and H. Liu, *Prog. Org. Coating*, 2021, **153**, 106137.
13 W. Jiang, A. Dai, T. Zhou and H. Xie, *Polym. Test.*, 2019, **80**, 106110.
14 G. Wu, D. Liu, J. Chen, G. Liu and Z. Kong, *Prog. Org. Coating*, 2019, **127**, 80–87.
15 H. Zhao, D. Huang, T.-H. Hao, G.-H. Hu, G.-b. Ye, T. Jiang and Q.-C. Zhang, *New J. Chem.*, 2017, **41**, 9268–9275.
16 X. Ji, H. Wang, X. Ma, C. Hou and G. Ma, *RSC Adv.*, 2017, **7**, 34086–34095.
17 H. Engels, H. Pirkl and R. Albers, *Angew. Chem., Int. Ed.*, 2013, **52**, 2–22.
18 H. Honarkar, *J. Dispersion Sci. Technol.*, 2018, **39**, 507–516.
19 S. M. Cakić, M. D. Valcic, I. S. Ristić, T. Radusin, M. J. Cvetinov and J. Budinski-Simendić, *Int. J. Adhes. Adhes.*, 2019, **90**, 22–31.
20 X. Cao, X. Ge, H. Chen and W. Li, *Prog. Org. Coating*, 2017, **107**, 5–13.
21 J. Li, W. Zheng, W. Zeng, D. Zhang and X. Peng, *Appl. Surf. Sci.*, 2014, **307**, 255–262.
22 Y. Meng, P. Lv, Q. Liu, B. Liao, H. Pang and W. Liu, *New J. Chem.*, 2019, **43**, 19193–19199.
23 S. Bhattarai, S. Lee, D. Lee and Y. Lee, *Bull. Kor. Chem. Soc.*, 2019, **40**, 1046–1049.
24 F. Bauer, U. Decker, K. Czihal, R. Mehnert, C. Riedel, M. Riemschneider, R. Schubert and M. R. Buchmeiser, *Prog. Org. Coating*, 2009, **64**, 474–481.
25 K. M. Zia, M. A. Iqbal, M. Zuber, M. Ishaq, M. A. Farrukh and M. N. Ahmad, *J. Elastomers Plastics*, 2014, **47**, 1–12.
26 Z. Cao, Q. Zhou, S. Jie and B. G. Li, *Ind. Eng. Chem. Res.*, 2016, **55**, 1582–1589.
27 Y.-H. Ge, J.-Y. Kang, J.-H. Zhou and L.-W. Shi, *Comput. Mater. Sci.*, 2016, **115**, 92–98.
28 M. Amrollahi and G. M. M. Sadeghi, *Prog. Org. Coating*, 2016, **93**, 23–33.
29 D. Nagle, M. Celina and L. Rintoul, *Polym. Degrad. Stab.*, 2007, **92**, 1446–1454.
30 Y. Luo, Y. Miao and F. Xu, *Macromol. Res.*, 2011, **19**, 1233–1241.
31 L. Wang, J. Li and H. Chen, *Paint Coating Ind.*, 2017, **47**, 6.
32 K. Malkappa, B. N. Rao and T. Jana, *Polymer*, 2016, **99**, 404–416.

© 2023 The Author(s). Published by the Royal Society of Chemistry